CAPÍTULO 1

INFLUENCE OF PUSH–PULL SUBSTITUENTS ON THE ELECTRONIC AND CHEMICAL REACTIVITY CHARACTERIZATION OF BENZOXAZOLE DERIVATIVES WITH OPTOELECTRONIC POTENTIAL

https://doi.org/10.22533/at.ed.666112610021

Edwin Smith Rivera Fernandez
Grupo de Espectroscopía Óptica y Láser -GEL, Universidad Popular del Cesar
Valledupar – Colombia
https://orcid.org/0000-0002-5572-3359

Romelio Jose Gonzalez Daza
Departamento de Matemáticas y Estadística, Universidad Popular del Cesar
Valledupar – Colombia
https://orcid.org/0009-0009-6279-7151

Lacides Alfonso Baleta Palomino
Departamento de Matemáticas y Estadística, Universidad Popular del Cesar
Valledupar – Colombia
https://orcid.org/0000-0002-3501-2365

Jader Enrique Esquivel Mojica
Departamento de Matemáticas y Estadística, Universidad Popular del Cesar
Valledupar – Colombia
https://orcid.org/0009-0008-9231-1354

Harold Valle Fuentes
Departamento de Matemáticas y Estadística, Universidad Popular del Cesar
Valledupar – Colombia
https://orcid.org/0000-0002-4450-3908

Gustavo Rodríguez pontón
Departamento de Matemáticas y Estadística, Universidad Popular del Cesar
Valledupar – Colombia
https://orcid.org/0009-0009-7210-3176

RESUMO: Este estudo concentra-se nas propriedades eletrônicas e na reatividade química intrínseca de quatro moléculas orgânicas derivadas do benzoxazol. A pesquisa também aborda o impacto do solvente polar metanol e do solvente não polar tolueno, bem como a influência de substituições que dão origem a efeitos de ressonância individuais e ao efeito push–pull simultâneo de substituintes, envolvendo um doador e um aceitador de elétrons. Os substituintes escolhidos incluem um fragmento do radical amino da amônia NH_2 e um fragmento do radical dióxido de nitrogênio NO_2. Utilizando o software Gaussian como ferramenta computacional no âmbito da Teoria do Funcional da Densidade (DFT), empregou-se o funcional de três parâmetros de Becke, Lee, Yang e Parr (B3LYP) juntamente com o conjunto de funções de base Gaussian Pople 6-31+G(d). Para simular as interações soluto–solvente, foi utilizado o modelo de contínuo polarizável (PCM). Nesse contexto, foi possível estimar as propriedades eletrônicas e a reatividade química intrínseca das moléculas derivadas do benzoxazol, destacando-se um resultado notável, especialmente para a molécula IV, tanto no solvente polar metanol quanto no tolueno. Sua constituição, que envolve simultaneamente fragmentos doadores e aceitadores de elétrons, induziu o efeito push–pull, resultando em uma diminuição da energia total, do gap de energia e da dureza molecular em ambos os solventes, além de um aumento da eletronegatividade, do comprimento de onda de transição e do momento dipolar. Em conclusão, as propriedades eletrônicas identificadas, quando comparadas com estudos semelhantes, sugerem a possível utilidade dessas moléculas orgânicas como camadas ativas em células solares, particularmente aquelas projetadas para absorver nas regiões violeta distante e azul. Além disso, sua aplicação em dispositivos OLED ou como novos meios ativos para lasers sintonizáveis nas regiões violeta e ultravioleta representa uma perspectiva promissora a ser explorada.

PALAVRAS-CHAVE: Propriedades eletrônicas, Teoria do Funcional da Densidade e Benzoxazol.

INFLUÊNCIA DE SUBSTITUINTES PUSH–PULL SOBRE A CARACTERIZAÇÃO ELETRÔNICA E DA REATIVIDADE QUÍMICA DE DERIVADOS DO BENZOXAZOL COM POTENCIAL OPTOELETRÔNICO

ABSTRACT: This study focuses on the electronic properties and intrinsic chemical reactivity of four organic molecules derived from benzoxazole. The research extends to the impact of both the polar solvent methanol and the non-polar solvent toluene; in addition, the impact of substitutions that give rise to individual resonance effects, as well as the simultaneous push-pull effect of substituents, one electron donor and one electron acceptor. The chosen substituents include a fragment of the

ammonia NH2 amino radical and a fragment of the nitrogen dioxide NO2 radical. Using Gaussian as a computational tool within the framework of density functional theory (DFT), we use the three-parameter functional of Becke, Lee, Yang and Parr (B3LYP) and the Gaussian Pople 6-31+g(d) base set. To simulate solute-solvent interactions, the polarizable continuum model (PCM) was used. In this context, it was possible to estimate the electronic properties and intrinsic chemical reactivity of the benzoxazole-derived molecules, highlighting a notable result, especially with molecule IV in both the polar solvent methanol and toluene. Its constitution, which simultaneously involves electron donor and acceptor fragments, induced the push-pull effect. This resulted in a decrease in energy, the energy gap and molecular hardness for both solvent cases, along with an increase in electronegativity, transition wavelength and dipole moment. In conclusion, the identified electronic properties, when compared with similar studies, suggest the possible utility of these organic molecules as active layers in solar cells, particularly those designed to absorb in the far violet and blue regions. In addition, their application in OLED devices or as new active media for tunable lasers in the violet and UV regions could be a promising avenue to explore.

KEYWORDS: Electronic properties, Density Functional Theory and Benzoxazole.

INTRODUCTION

Organic compounds (COs) composed of organic molecules with pi-conjugated bonds are interesting because their multiple applications are related to and depend on the optical and electronic properties, as well as the photostability of these substances(Liu et al., 2020). These are studied within the field of laser physics and optical spectroscopy to provide possible solutions to the still existing need to cover the widest possible optical spectral range through the laser effect(Rivera et al., 2020). On the other hand, OLEDs are diodes made up of thin films of OCs that react to certain electrical stimuli, producing light emission(EL Mhamedi et al., 2025). Their applications are envisioned in the manufacture of flexible, high-resolution, large-scale screens that are desired to be improved, as there has been an increased demand in the market for extra-large screens with multiple functions(Chemek et al., 2023).

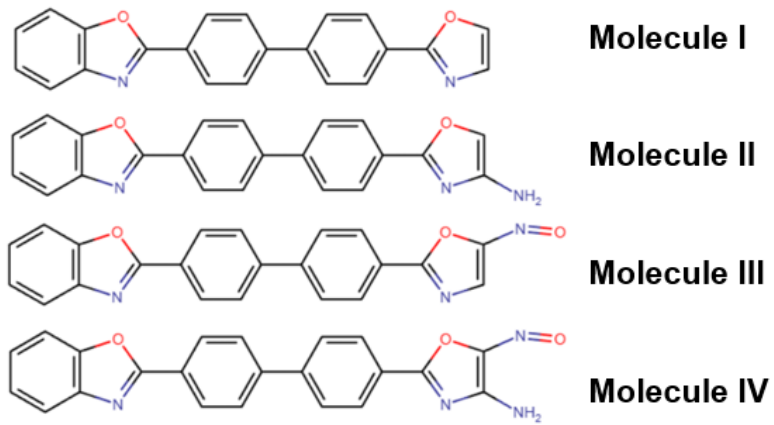

Figure 1. *Molecular structures studied.*

Renewable energies, such as solar energy, are optimal alternatives to replace highly polluting hydrocarbons, so the search for new photovoltaic materials is considered a necessity and provides new horizons for COs, which can be used as active layers of photovoltaic cells, as they offer very low manufacturing costs, and are lightweight and flexible materials(Waqas et al., 2025).

In this context, the electronic properties and intrinsic chemical reactivity of four COs (see Figure 1) with a single ring chain structure were designed, modeled, and compared in the polar solvent methanol and in the nonpolar solvent toluene, with the purpose of: (1) investigating the potential use of these compounds as organic light-emitting diodes, active layers for solar cells, or active media for tunable lasers, (2) investigating the influence of the polar solvent methanol and nonpolar toluene, and, (3) investigating the resonant charge transfer effect of electrodonor and electroacceptor fragments, individually, and based on the positive and negative effect simultaneously on the molecular electronic properties and intrinsic chemical reactivity.

The results obtained are relevant for the interpretation of the behavior of these compounds based on the global electronic properties and intrinsic chemical reactivity, based on the global molecular descriptors such as the total energy of each of the systems, the dipole moment, the molecular hardness, the electronegativity, the frontier orbitals HOMO and LUMO, the energy gap and the transition wavelength of the gap, where all this information is necessary to predict and identify the spectral absorption and emission centers.

THEORETICAL FOUNDATIONS AND COMPUTATIONAL DETAILS

Predicting from the modeling of the electronic properties and intrinsic chemical reactivity of any molecular system is useful for foreseeing the optical behavior of organic substances due to the individual and group behavior of the molecules that constitute them(Idrissi et al., 2021). Density functional theory is a theory that unifies much of the local and global descriptors of the molecular systems of interest. Using the Kohn-Sham potential energy in DFT(Islam et al., 2025), where the total energy of the system is expressed as an electronic density functional, is described in the following equation:

$$E[\rho(r)] = F[\rho(r)] + \int v(r)\rho(r)d\tau$$

where F is the universal Hohenberg–Kohn functional and $v(r)$ is the potential resulting from internal interactions between the atoms of the molecule, as well as external interactions with the molecules that constitute the solvent.

According to the theory of Pearson and Parr (Hirata, 2025), the chemical potential μ) and chemical hardness (η) can be obtained using Koopmans' theorem and the finite difference approximation, based on the energies of the frontier molecular orbitals, HOMO (E_H) and LUMO (E_L). These quantities are defined by the following expressions:

$$\mu = \frac{1}{2}(E_L + E_H)$$

And

$$\eta = \frac{1}{2}(E_L - E_H)$$

The electronegativity (χ) is obtained by associating the chemical potential with hardness, leading to the electrophilicity expression:

$$\chi = \frac{\mu^2}{2\eta}$$

These principles allow the characterization of the electronic properties and intrinsic chemical reactivity of the molecules under study, based on parameters such as total energy, dipole moment, electronegativity, frontier molecular orbitals, energy gap, and the transition wavelength between the gap orbitals.

All calculations were performed using the Gaussian 09 software package within the framework of density functional theory (DFT)(Deringer et al., 2021). The hybrid B3LYP functional and the 6-31+G(d) basis set were employed(Nakata & Maeda, 2023). To describe the interactions between the molecules and the polar solvent methanol, the polarizable continuum model (PCM) was used(Severoglu et al., 2025).

RESULTS

Electronic properties and intrinsic chemical reactivity of the molecular structures under study in methanol (polar solvent).

Molecular Descriptors	I	II	III	IV
Energy (eV)	–30117.25	–31623.66	–35682.34	–37188.99
		–5.00%	–18.48%	–23.48%
Dipole Moment (Debye)	3.57	6.01	9.63	14.23
		68.13%	169.48%	298.13%
Homo (eV)	–6.06	–5.68	–6.16	–6.07
		6.36%	–1.60%	–0.04%
Lumo (eV)	–2.12	–2.11	–3.19	–2.84
		0.47%	–50.46%	–33.81%
Energy Gap ΔE_g (Ev)	3.94	3.57	2.97	3.23
		–9.52%	–24.66%	–18.12%
Electronegativity (χ)	4.09	3.89	4.68	4.45
		–4.83%	14.25%	8.78%
Molecular Hardness (H)	1.97	1.78	1.49	1.61
		–9.52%	–24.66%	–18.12%
Transition Wavelength ΔE_g (nm)	314.76	347.88	417.81	384.40
		10.52%	32.74%	22.12%
Spectral Frequency ν (nm^{-1})	0.32	0.29	0.24	0.26
		–9.52%	–24.66%	–18.12%
Spectral Shift (nm)	0.00	33.12	103.05	69.64

Table 1. Molecular descriptors of benzoxazole derivatives in methanol.

Interpretation of the Energy Values

Table 1 presents the energy results obtained for the molecular structures under study, which were analyzed in a polar solvent, namely methanol. It should be recalled that the main molecule, referred to as the parent molecule, is molecule I, whose energy value is –30117.25 eV. For molecule II, the calculated energy was –31623.25 eV; therefore, the energy of molecule II decreased by 5% compared to that of the parent molecule. For molecular structure III, the energy was –35682.34 eV, which is 18.48% lower than the energy of the parent molecule and also lower than that of derived molecule II. For molecular structure IV, the calculated energy was –37188.99 eV, indicating a reduction of 23.48% compared to the energy of the parent molecular structure.

From the calculated energy results for each derived molecular structure, it can be observed that, in all cases, the energy value decreases when compared with that of the parent molecule. Among them, molecule IV exhibits the lowest energy, while molecule II presents the highest energy among the derivatives. This decrease in energy values observed for each derived molecule is attributed to the modification of the electronic system of the parent molecule (Molecule I) through mono- or disubstitution, which increases the number of atoms and, consequently, the number of electrons in the derived molecules.

Interpretation of the Dipole Moment

The dipole moment of a molecule is an electronic property that provides a measure of the asymmetry of the charge distribution within the molecule. As shown in Table 1, the dipole moment of the parent molecule is 3.57 D. For derived molecular structure II, the calculated dipole moment is 6.01 D, representing an increase of 68.13% compared to the parent molecule. In the case of molecule III, the dipole moment is 6.63 D, corresponding to an increase of 169.48% relative to the parent structure. In addition, molecule III exhibits a higher dipole moment than molecule II, which is attributed to the influence of the nitro group acting as an electron acceptor, facilitating electron displacement from the primary molecular block toward the substituent. In contrast, molecule II contains an electron-donating amino group, which promotes electron density transfer from the donor fragment toward the primary molecular block.

For molecule IV, the dipole moment reaches 14.23 D, representing an increase of 298.13% compared to the parent molecule. This significant enhancement is associated with the push–pull effect resulting from the simultaneous presence of an electron-donating amino group (NH_2) and an electron-accepting nitro group (NO_2), which induces a strong intramolecular charge redistribution.

Frontier Molecular Orbitals

Regarding the HOMO energy, the parent molecule exhibits a value of –6.06 eV. For the derived structures, the HOMO energies are –5.68 eV for molecule II, corresponding to an increase of 6.36%, –6.16 eV for molecule III, representing a slight decrease of 1.60%, and –6.07 eV for molecule IV, showing a negligible decrease of 0.04% compared to the parent molecule.

The LUMO energy of the parent molecule is –2.12 eV. For molecule II, the LUMO energy is –2.11 eV, showing a marginal increase of 0.47%. In contrast, molecule III exhibits a significant stabilization of the LUMO at –3.19 eV, corresponding to a decrease of 50.46%, while molecule IV shows a LUMO energy of –2.84 eV, decreasing by 33.81% relative to the parent molecule.

Energy Gap

The calculated energy gap for the parent molecule in methanol is 3.94 eV. Among the derived structures, molecule III shows the largest reduction in the energy gap, reaching 2.97 eV, which corresponds to a decrease of 24.66%. Molecule II presents an energy gap of 3.57 eV, decreasing by 9.52%, while molecule IV exhibits a gap of 3.23 eV, corresponding to a reduction of 18.12% relative to the parent molecule.

The observed reduction in the energy gap for the derived molecules arises from the contribution of electron-donating and electron-accepting substituents, either through monosubstitution or through the simultaneous push–pull effect in molecule IV. These electronic modifications reduce the energy required for electronic transitions from the HOMO to the LUMO, allowing the prediction of a bathochromic shift in the absorption spectra of the derived structures.

Interpretation of Electronegativity (χ)

Electronegativity represents the ability of a molecular system to attract electrons. The electronegativity of the parent molecule is 4.09. For molecule II, this value decreases to 3.89, corresponding to a reduction of 4.83%, which can be attributed to the presence of an electron-donating amino group that supplies electron density to the molecular framework.

In contrast, molecule III exhibits an increase in electronegativity to 4.68, representing a rise of 14.25% relative to the parent molecule. This behavior is explained by the electron-withdrawing nature of the nitro group, which enhances the molecule's tendency to attract electrons. For molecule IV, the electronegativity increases to 4.45, corresponding to an increase of 8.78%. However, this increase is smaller than that observed for molecule III due to the simultaneous presence

of electron-donating and electron-accepting substituents, clearly evidencing the push–pull effect.

Interpretation of Molecular Hardness (η)

Molecular hardness is a global descriptor that measures the resistance of a molecule to changes in its electronic distribution. The parent molecule exhibits a hardness of 1.97. For the derived molecules, the hardness values are 1.78 for molecule II, 1.49 for molecule III, and 1.61 for molecule IV, corresponding to reductions of 9.52%, 24.66%, and 18.12%, respectively. These results indicate that substitution significantly reduces molecular hardness, with the electron-accepting nitro group producing the strongest effect. Although the push–pull effect might be expected to increase hardness, molecule IV does not exceed the reduction observed for molecule III, where only the nitro group is present.

Transition Wavelength (λ_G)

For the parent molecule, an electronic transition from the HOMO to the LUMO requires excitation by a photon with a wavelength of 314.76 nm. For molecule II, this transition occurs at 347.88 nm, representing an increase of 10.52%. Molecule III requires a wavelength of 417.81 nm, corresponding to an increase of 32.74%, while molecule IV exhibits a transition wavelength of 384.40 nm, representing an increase of 22.12% relative to the parent molecule.

Spectral Frequency ($\tilde{\nu}$)

Based on the transition wavelengths, the spectral frequency required to excite an electron from the HOMO to the LUMO is 0.32 nm^{-1} for the parent molecule. For molecule II, the required frequency decreases to 0.29 nm^{-1}, representing a reduction of 9.52%. Molecule III requires a frequency of 0.24 nm^{-1}, corresponding to a reduction of 24.66%, while molecule IV exhibits a frequency of 0.26 nm^{-1}, decreasing by 18.12% relative to the parent structure.

Spectral Shift

The difference between the transition wavelengths of the derived molecules and that of the parent molecule (314.76 nm) corresponds to the spectral shift. The calculated spectral shifts are 33.12 nm for molecule II, 103.05 nm for molecule III, and 69.64 nm for molecule IV. These results indicate that molecule III exhibits the largest spectral shift relative to the parent molecule, followed by molecule IV and molecule II. This behavior is primarily attributed to the strong electron-accepting character of the nitro group, whereas the amino substitution and the push–pull effect lead to comparatively smaller spectral shifts.

Electronic properties and intrinsic chemical reactivity of the molecular structures under study in Toluene (non-polar solvent)

Molecular Descriptors	I	II	III	IV
Energy (eV)	-30117,10	-31623,46	-35682,12	-37188,67
		-5,00%	-18,48%	-23,48%
Dipole Moment (Debye)	2,83	4,82	8,02	11,40
		70,58%	183,70%	303,24%
Homo (eV)	-6,00	-5,64	-6,15	-6,08
		5,90%	-2,54%	-1,41%
Lumo (eV)	-2,03	-2,01	-3,09	-2,65
		0,95%	-52,14%	-30,75%
Energy Gap ΔE_g (Ev)	3,97	3,63	3,06	3,43
		-8,43%	-22,84%	-13,60%
Electronegativity (χ)	4,01	3,83	4,62	4,37
		-4,65%	15,09%	8,83%
Molecular Hardness (H)	1,98	1,82	1,53	1,71
		-8,43%	-22,84%	-13,60%
Transition Wavelength ΔE_g (nm)	312,99	341,81	405,66	362,27
		9,21%	29,61%	15,75%
Spectral Frequency ν (nm^{-1})	0,32	0,29	0,25	0,28
		-8,43%	-22,84%	-13,60%
Spectral Shift (nm)	0,00	28,82	92,67	49,28

Table 2. Molecular descriptors of benzoxazole derivatives in Toluene.

Interpretation of the Energy Values

Table 2 shows the computational results for the molecular structures under study in the liquid phase, using a non-polar solvent, namely toluene. Among them, molecule I should be highlighted because it corresponds to the parent molecular structure, whose energy was calculated as –30117.10 eV. For molecule II, the energy was calculated as –31623.46 eV, indicating that it decreased by 5% compared to the energy of the parent molecule. For molecular structure III, the calculated energy was –35682.12 eV, being 18.48% higher than the energy of the parent molecule and also higher than the energy of derived molecule II. For molecular structure IV, the total energy is –37188.67 eV; therefore, it can be stated that it decreased by 23.48% compared with the energy of the parent molecular structure.

This highlights the influence of the amino group (–NH2) in the ortho position for molecule II and the nitro group (NO2) in the para position for molecule III, as well as the presence of both substitutions in derived molecule IV, which makes the total energy much higher than the total energy of the parent molecule and the other derivatives under study. Nevertheless, the energy results for each derived structure decreased relative to the parent structure, with molecule IV showing the lowest energy and molecule II the highest energy among the derivatives.

Interpretation of the Dipole Moment

The dipole moment provides a measure of the asymmetry of the charge distribution within a molecule and, therefore, reflects the average magnitude of attractive forces between atoms. For the parent molecule, the dipole moment is 2.83 D. For derived molecular structure II, the calculated dipole moment is 4.82 D, indicating an increase of 70.58% compared to the parent structure. For molecule III, the dipole moment is 8.02 D, meaning that it increased by 183.7% relative to the parent structure. Moreover, for molecule IV, the dipole moment is 1.4 D, increasing by 303.24% compared to the parent molecule.

It is evident that molecule III exhibits a higher dipole moment than molecule II, which is attributed to the influence of the nitro group in molecule III, enabling electron displacement from the primary molecular block toward the nitro electron-acceptor fragment. In contrast, for molecule II, the presence of an amino fragment leads to an electronic distribution in which electron density is donated by the amino donor group. Likewise, when the dipole moment of molecule IV is compared with those of molecules II and III, a marked increase is observed. This indicates that the push–pull effect provides the pronounced increase in the dipole moment of derived molecule IV compared with the other molecular structures studied in non-polar toluene.

Frontier Molecular Orbitals

Regarding the HOMO frontier orbital, as shown in Table 2, the parent molecule presents a HOMO energy of –6.0 eV. For molecule II, the HOMO energy is –5.64 eV, representing an increase of 5.9% relative to the HOMO of the parent molecule. For molecule III, the HOMO energy is –6.15 eV, decreasing by 2.54% with respect to the parent molecule. For molecule IV, the HOMO energy is –6.08 eV, showing only a 1.41% decrease relative to the parent molecule.

For the LUMO frontier orbital, Table 2 shows a value of –2.03 eV for the parent molecule. In molecule II, the LUMO energy is –2.01 eV, which represents a slight increase of 0.95% compared to the parent LUMO. For molecule III, the LUMO energy is –3.09 eV, being 52.14% lower than the LUMO of the parent molecule. For molecule

IV, the LUMO energy is –2.65 eV; therefore, it decreased by 30.75% relative to the energy of the parent LUMO.

Concerning the energy gap, Table 2 shows that the parent molecular structure exhibits an energy gap of 3.63 eV. For molecule II, the energy gap decreased by 8.43% compared to the parent structure. For molecule III, the energy gap is 3.06 eV, corresponding to a decrease of 22.84% relative to the parent molecule. For derived molecule IV, the energy gap is 3.43 eV, indicating a decrease of 16.60% compared to the parent molecule.

The reduction in the energy gap observed for the derived structures in toluene, compared with the energy gap of the parent molecule (also in toluene), results from the contribution of electrons introduced by electron-donating and electron-accepting fragments, and simultaneously through the push–pull effect, into the molecular electronic systems under study. Therefore, a bathochromic shift can be predicted for each derived structure, corresponding to a displacement of the absorption spectrum toward longer wavelengths (lower-energy photons), associated with HOMO-to-LUMO transitions.

Interpretation of Electronegativity (χ)

Table 2 shows that the electronegativity of the parent molecule is 4.01, which is higher than the electronegativity of molecule II. In molecule II, electronegativity decreases by 4.65% relative to the parent structure due to the electron donation from the amino fragment to the molecular framework. The same table also shows that the electronegativities of derived molecules III and IV are higher than that of the parent structure, with values of 4.62 and 4.37, respectively. This increase is attributed to the contribution of the electron-accepting nitro group in molecules III and IV. However, the increase in electronegativity for molecule III is larger than that for molecule IV: relative to the parent molecule, molecule III increases by 15.09%, whereas molecule IV increases by 8.83%.

Therefore, it should be highlighted that the nitro group (NO2) produces a considerable increase in electronegativity in derived structures III and IV, and that substitution with the nitro fragment alone increases electronegativity more strongly than when it acts simultaneously with an electron-donating fragment that generates a push–pull effect. Consequently, molecule III exhibits the greatest ability to attract electrons, molecule II exhibits the lowest electron-attracting ability, and molecule IV, although it has a higher electron-attracting capacity than the parent molecule and molecule II, remains below that of molecule III.

Interpretation of Molecular Hardness (η)

The molecular hardness results for the structures under study are presented in Table 2. A value of 1.98 was obtained for the parent molecule, 1.82 for derived molecule II, 1.53 for derived molecule III, and 1.71 for derived molecule IV. Thus, molecular hardness decreases for molecules II, III, and IV relative to the parent molecule by 8.43%, 22.84%, and 13.60%, respectively.

These results indicate that both monosubstitution and disubstitution decrease the molecular hardness of the derived structures compared to the parent, due to the increased electron density introduced into the parent molecular system. The nitro electron-acceptor group (NO2) produces the strongest reduction in this property, as observed for monosubstituted molecule III and disubstituted molecule IV. It should be noted that although molecular hardness decreases in both monosubstitutions (molecules II and III), the result for molecule IV is not additive; rather, it lies below the average of the hardness decreases observed for molecules II and III.

Transition Wavelength ()

To achieve an electronic transition in the parent molecular structure from the HOMO to the LUMO, excitation with a photon of wavelength 312.99 nm is required. If the same process is to occur in molecular structures II, III, and IV, photons with wavelengths of 341.81 nm, 405.66 nm, and 362.27 nm are required, respectively. This indicates that, compared with the parent structure, the transition wavelengths increase by 9.21%, 29.61%, and 15.75% for derived molecules II, III, and IV, respectively.

Therefore, it is evident that monosubstitution with the electron-donating amino group (NH2), monosubstitution with the electron-accepting nitro group (NO2), and the simultaneous disubstitution with both donor and acceptor fragments (NH2 and NO2) not only influence the frontier orbitals and the other molecular descriptors, but also affect the energy (energy gap) required for the transition and, consequently, the wavelength of the photon needed to promote the HOMO–LUMO transition.

Spectral Frequency ($\tilde{\nu}$)

When an electronic transition between the HOMO and LUMO frontier orbitals is possible for the molecular structures under study, the photon must have a spectral frequency that can be obtained from the transition wavelength and, consequently, from the energy gap. For the parent molecule, the required spectral frequency is 0.32 $nm^{-}1$, while for the derived molecules it is 0.29 $nm^{-}1$, 0.25 $nm^{-}1$, and 0.28 $nm^{-}1$, respectively. These values represent reductions of 8.43% for molecule II, 22.84% for molecule III, and 13.6% for molecule IV, all relative to the parent molecule. Therefore, if the parent molecule undergoes a HOMO-to-LUMO transition, excitation would

require a photon with a frequency of 0.32 nm¯1, and analogous reasoning applies to the derived molecules.

Spectral Shift

The spectral shift is defined as the difference between the transition wavelength of the derived molecular structures and that of the parent structure. For molecule II, the spectral shift is 28.82 nm; for molecule III, it is 92.67 nm; and for molecule IV, it is 49.28 nm. Thus, molecule III exhibits the largest spectral shift compared with molecules II and IV.

This larger spectral shift in molecule III is enabled by the strong influence of the nitro fragment (NO2) on the parent structure, whereas the amino group and the push–pull effect in molecules II and IV produce substantially smaller spectral shifts.

DISCUSSION

The results obtained for benzoxazole derivatives in methanol and toluene reveal a clear correlation between the nature of the substituents, the solvent environment, and the global electronic properties of the molecules, which is decisive for their potential application in optoelectronic devices.

First, the progressive decrease in total energy from the parent molecule (I) to the derived molecules—particularly for molecule IV (–37188.99 eV in methanol and –37188.67 eV in toluene)—indicates significant substitution-induced electronic stabilization. This behavior has been reported in previous studies on donor–acceptor systems based on benzoxazole and benzimidazole, where the incorporation of electron-accepting groups such as $–NO_2$ and push–pull combinations leads to electronically more stable systems with enhanced effective conjugation(Kong et al., 2026). From an application standpoint, such stabilization is relevant for active materials in organic solar cells (OSCs), as lower total energy is often associated with greater thermal and photochemical stability under continuous operation(Maadh et al., 2024).

The dipole moment exhibits one of the most functionally relevant effects. In methanol, the dipole moment increases from 3.57 D for the parent molecule to 14.23 D for molecule IV, while in toluene it increases from 2.83 D to 11.40 D. Dipole moments exceeding 10 D have been associated in the literature with strong intramolecular charge separation and pronounced intramolecular charge-transfer (ICT) carácter (Benhafsa et al., 2025). Such behavior is highly desirable in photovoltaic materials and OLEDs, as it promotes exciton dissociation and directional charge transport(Wang et al., 2023). Experimental and theoretical studies on push–pull chromophores report that dipole moments in the range of 8–15 D often correlate with improved

charge-separation efficiency and enhanced nonlinear optical response, positioning molecule IV as a particularly attractive candidate.

Analysis of the frontier molecular orbitals confirms that the main substitution-induced electronic modifications are manifested in the stabilization of the LUMO (Thanmayalaxmi et al., 2024). In methanol, the LUMO of molecule III is stabilized to –3.19 eV, compared with –2.12 eV for the parent molecule, corresponding to a 50.46% decrease. This value is comparable to LUMO levels reported for organic acceptors used in solar cells, which typically lie between –3.0 and –4.0 eV. Molecule IV also exhibits significant LUMO stabilization (–2.84 eV), accompanied by an almost unchanged HOMO, enabling favorable tuning of the energy gap without compromising the stability of the occupied orbital.

The reduction of the HOMO–LUMO gap is another key result. In methanol, the gap decreases from 3.94 eV for the parent molecule to 2.97 eV for molecule III and 3.23 eV for molecule IV. A similar trend is observed in toluene, with gaps of 3.06 eV and 3.43 eV for molecules III and IV, respectively. These values fall within the range reported for organic materials used in violet–blue emitting devices and in wide-bandgap OSC active layers. In particular, gaps close to 3.0 eV are suitable for absorbers in the blue region, which coincides with the spectral region of interest for blue OLEDs—an area that remains technologically challenging due to stability and efficiency issues (Mahmoudi et al., 2022).

The transition wavelengths reinforce this interpretation. In methanol, molecule III exhibits a transition at 417.81 nm and molecule IV at 384.40 nm, evidencing a clear bathochromic shift relative to the parent molecule (314.76 nm). Shifts exceeding 80–100 nm, such as that observed for molecule III, have been reported in systems with strong donor–acceptor character and are associated with extended π-conjugation and charge-transfer excited states. These displacements make molecules III and IV particularly attractive for optical absorption in the violet and blue regions of the visible spectrum, both for photovoltaic devices and electroluminescent emitters.

Electronegativity and molecular hardness complete the functional picture. Molecule III exhibits the highest electronegativity (4.68 in methanol and 4.62 in toluene) and the lowest hardness (1.49 in methanol and 1.53 in toluene), indicating a high electron-accepting capability and greater ease of electronic redistribution. These features are consistent with acceptor materials or active components in organic heterojunctions. By contrast, molecule IV presents a more balanced combination of electronegativity and hardness, which is characteristic of push–pull systems designed to combine efficient absorption with balanced charge transport (Ullah et al., 2025).

CONCLUSIONS

The theoretical study carried out using DFT/B3LYP enabled a systematic characterization of the electronic properties and intrinsic chemical reactivity of four benzoxazole derivatives in polar (methanol) and non-polar (toluene) solvent environments. The results show that electronic substitutions exert a decisive influence on global molecular descriptors, particularly total energy, dipole moment, electronegativity, molecular hardness, and the HOMO–LUMO gap. In both solvents, a progressive energetic stabilization was observed when moving from the parent molecule to the derived structures, with molecule IV being the most stabilized. This behavior is associated with the simultaneous presence of electron-donating and electron-accepting fragments that induce a pronounced push–pull effect. Furthermore, the stabilization of the LUMO orbital and the reduction of the energy gap, especially in molecules III and IV, confirmed the ability of these structural modifications to favor lower-energy electronic transitions and to generate significant bathochromic shifts.

From an application perspective, the electronic properties obtained position the studied benzoxazole derivatives as promising candidates for optoelectronic applications. In particular, the high dipole moment values, the reduction in molecular hardness, and energy gaps close to 3.0 eV, together with optical transitions in the violet–blue region, are consistent with the requirements of active materials in wide-bandgap organic solar cells and blue-emitting OLED devices. Molecule IV stands out by exhibiting a favorable balance between charge transfer, electronic stability, and energy-gap tuning, making it an especially attractive system for the design of photovoltaic and emissive active layers. Additionally, the observed spectral shifts and the consistent response in both solvents suggest that these systems could be explored as active media in tunable lasers operating in the violet and near-ultraviolet regions, opening new perspectives for the rational development of functional organic materials based on benzoxazole.

REFERENCES

Benhafsa, L. M., Azzaz, Y., Benseddik, N., Moulay, N., Bensaid, D., & Bencherif, K. (2025). Optoelectronic and Photovoltaic Properties of Lead-Free Ba2AgBiX6 (X=I, Br and Cl) Double Perovskites: As a Sustainable Solar Cell Study Based on DFT and SCAPS-1D. *Journal of Inorganic and Organometallic Polymers and Materials 2025*, 1–16. https://doi.org/10.1007/S10904-025-04014-W

Chemek, M., Braiek, M. Ben, Mabrouk, A., Wazzan, N., Mansour, A. Ben, Hafiane, O., & Kamel, A. (2023). Optoelectronic properties of a new luminescent-synthesized organic material based on carbazole and thiophene rings for a new generation of OLEDs devices: experimental investigations and DFT modeling. *Journal of Materials Science: Materials in Electronics*, *34*(24), 1–12. https://doi.org/10.1007/S10854-023-11068-4/TABLES/4

Deringer, V. L., Bartók, A. P., Bernstein, N., Wilkins, D. M., Ceriotti, M., & Csányi, G. (2021). Gaussian Process Regression for Materials and Molecules. *Chemical Reviews*, *121*(16), 10073–10141. https://doi.org/10.1021/ACS.CHEMREV.1C00022

EL Mhamedi, I., EL Malki, Z., & Bouachrine, M. (2025). Theoretical investigation of electro-optical properties of novel D-Pi-D based organic compounds for OLED applications. *Optical and Quantum Electronics*, *57*(3), 168. https://doi.org/10.1007/s11082-025-08086-3

Hirata, S. (2025). New Dimension in Ab Initio Electronic Structure Theory: Temperature, Pressure, and Chemical Potential. *The Journal of Physical Chemistry Letters*, *16*(15), 3632–3645. https://doi.org/10.1021/ACS.JPCLETT.5C00631

Idrissi, S., Labrim, H., Bahmad, L., & Benyoussef, A. (2021). DFT and TDDFT studies of the new inorganic perovskite CsPbI3 for solar cell applications. *Chemical Physics Letters*, *766*, 138347. https://doi.org/10.1016/J.CPLETT.2021.138347

Islam, M. A., Hossain, N., Ahsan, Z., Rana, M., Rahman, M., & Abdullah, M. (2025). DFT insights into the mechanical properties of NMs. *Results in Surfaces and Interfaces*, *18*, 100417. https://doi.org/10.1016/J.RSURFI.2025.100417

Kong, R., Zhu, Z., Duan, Y., Li, F., & Wang, H. (2026). An ab initio kinetic study on H-abstraction reactions from methyl butenoates by NO2. *Fuel*, *408*, 137576. https://doi.org/10.1016/J.FUEL.2025.137576

Liu, D., Sa, R., Wang, J., & Wu, K. (2020). Electronic and Optical Properties of Organic–Inorganic MASn1–xGexI3 Perovskites: A First-Principles Study. *Journal of Cluster Science*, *31*(5), 1103–1109. https://doi.org/10.1007/s10876-019-01718-1

Maadh, F. N., Abdulmalek, E., Ismail, M. F., Ahmad, S. A. A., & Abdulkreem-Alsultan, G. (2024). Recent Progress in Benzimidazole and Quinoxaline Dyes Based on Dye-Sensitized Solar Cells: A Comprehensive Overview. *High Energy Chemistry 2024 58:1*, *58*(1), 16–58. https://doi.org/10.1134/S0018143924010132

Mahmoudi, C., Chouk, R., Baatout, K., Jaballah, N. S., Khalfaoui, M., & Majdoub, M. (2022). Synthesis, characterization and DFT study of new anthracene-based semiconducting polyethers for OLED application. *Journal of Molecular Structure*, *1251*, 131993. https://doi.org/10.1016/J.MOLSTRUC.2021.131993

Nakata, M., & Maeda, T. (2023). PubChemQC B3LYP/6-31G*//PM6 Data Set: The Electronic Structures of 86 Million Molecules Using B3LYP/6-31G* Calculations. *Journal of Chemical Information and Modeling*, *63*(18), 5734–5754. https://doi.org/10.1021/ACS.JCIM.3C00899/ASSET/IMAGES/MEDIUM/CI3C00899_0035.GIF

Rivera, E. S., Avila, O. I., & Neira, O. L. (2020). Theoretical description of the electronic properties and intrinsic chemical reactivity of organic compounds derived from 1,3-Benzoxazole. *Journal of Physics: Conference Series*, *1547*(1), 012025. https://doi.org/10.1088/1742-6596/1547/1/012025

Severoglu, Y. B., Yuksel, B., Sucu, C., Aral, N., Uversky, V. N., & Coskuner-Weber, O. (2025). Implicit Solvent Models and Their Applications in Biophysics. *Biomolecules*, *15*(9), 1218. https://doi.org/10.3390/BIOM15091218

Thanmayalaxmi, D., Suvitha, A., Sakthivel, P., Alharbi, N., Florence, S., Trilaksana, H., & El-Mansy, M. A. M. (2024). Quantum Computational and Spectroscopic Investigation (UV), MEP, HOMO-LUMO, Pharmacokinetic Studies of Meloxicam: A DFT Study. *Springer Proceedings in Physics*, *414 SPP*, 91–101. https://doi.org/10.1007/978-3-031-69970-2_8

Ullah, A., Ibrahim, M., Yousuf, A., Ali, M. A., Xu, H. L., & Arshad, M. (2025). Crafting optical wonders: The interplay of electron push–pull dynamics and π-conjugation in non–linear optics. *Next Materials*, *9*, 101239. https://doi.org/10.1016/J.NXMATE.2025.101239

Wang, J. M., Lee, T. C., Chung, C. C., Chen, W. Y., Wu, S. Y., Lin, Y. D., Chang, Y. J., Lu, C. W., & Chang, C. H. (2023). Toward ultra-high efficiency tandem OLEDs: Benzothiazole-based bipolar hosts and specific device architectures. *Chemical Engineering Journal*, *472*, 145023. https://doi.org/10.1016/J.CEJ.2023.145023

Waqas, M., Khadka, D. B., Khan, A. H. H., & Wang, Y. C. (2025). Fullerene-driven photocarrier processes in perovskite solar cells: recent advances. *Nanoscale*, *17*(26), 15648–15675. https://doi.org/10.1039/D5NR01894C